

Source Echo Chamber: Exploring the Escalation of Source Bias in User, Data, and Recommender System Feedback Loop

Yuqi Zhou
Sunhao Dai
Gaoling School of Artificial Intelligence
Renmin University of China
Beijing, China
{yuqizhou,sunhaodai}@ruc.edu.cn

Liang Pang
CAS Key Laboratory of AI Safety
Institute of Computing Technology, CAS
Beijing, China
pangliang@ict.ac.cn

Gang Wang
Zhenhua Dong
Huawei Noah's Ark Lab
Shenzhen, China
wanggang110@huawei.com
dongzhenhua@huawei.com

Jun Xu
Gaoling School of Artificial Intelligence
Renmin University of China
Beijing, China
junxu@ruc.edu.cn

Ji-Rong Wen
Gaoling School of Artificial Intelligence
Renmin University of China
Beijing, China
jirong.wen@gmail.com

ABSTRACT

Recently, researchers have uncovered that neural retrieval models prefer AI-generated content (AIGC), called **source bias** [10, 40]. Compared to active search behavior, recommendation represents another important means of information acquisition, where users are more prone to source bias. Furthermore, delving into the recommendation scenario, as AIGC becomes integrated within the feedback loop involving users, data, and the recommender system, it progressively contaminates the candidate items, the user interaction history, and ultimately, the data used to train the recommendation models. How and to what extent the source bias affects the neural recommendation models within feedback loop remains unknown. In this study, we extend the investigation of source bias into the realm of recommender systems, specifically examining its impact across different phases of the feedback loop. We conceptualize the progression of AIGC integration into the recommendation content ecosystem in three distinct phases-HGC dominate, HGC-AIGC co-exist, and AIGC dominance-each representing past, present, and future states, respectively. Through extensive experiments across three datasets from diverse domains, we demonstrate the prevalence of source bias and reveal a potential digital **echo chamber** with source bias amplification throughout the feedback loop. This trend risks creating a recommender ecosystem with limited information source, such as AIGC, being disproportionately recommended. To counteract this bias and prevent its escalation in the feedback loop, we introduce a black-box debiasing method that maintains model impartiality towards both HGC and AIGC. Our experimental results validate the effectiveness of the proposed debiasing method, confirming its potential to disrupt the feedback loop.

Permission to make digital or hard copies of all or part of this work for personal or classroom use is granted without fee provided that copies are not made or distributed for profit or commercial advantage and that copies bear this notice and the full citation on the first page. Copyrights for components of this work owned by others than ACM must be honored. Abstracting with credit is permitted. To copy otherwise, or republish, to post on servers or to redistribute to lists, requires prior specific permission and/or a fee. Request permissions from [permissions@acm.org](https://permissions.acm.org).

Conference acronym 'XX, June 03–05, 2018, Woodstock, NY

© 2018 Association for Computing Machinery.
ACM ISBN 978-1-4503-XXXX-X/18/06...\$15.00
<https://doi.org/XXXXXXXXXXXXXX>

ACM Reference Format:

Yuqi Zhou, Sunhao Dai, Liang Pang, Gang Wang, Zhenhua Dong, Jun Xu, Ji-Rong Wen. 2018. Source Echo Chamber: Exploring the Escalation of Source Bias in User, Data, and Recommender System Feedback Loop. In *Woodstock '18: ACM Symposium on Neural Gaze Detection, June 03–05, 2018, Woodstock, NY*. ACM, New York, NY, USA, 14 pages. <https://doi.org/XXXXXXXXXXXXXX>

1 INTRODUCTION

The development of Large Language Models (LLMs) is advancing rapidly [45], demonstrating strong capabilities and performing excellently in many text generation tasks, such as machine translation [20], summarization [43], and complex question answering [30, 41]. Due to the cost-effectiveness, high quality, and speed of generating Artificial Intelligence Generated Content (AIGC) compared to Human Generated Content (HGC), an increasing volume of online content is being produced by these models. This shift is altering the existing content creation paradigm and resulting in a notable prevalence of AIGC on the internet [9]. In retrieval systems, these abundant AIGCs are more likely to be ranked higher in the candidate items set by the neural retrievals, a phenomenon known as **source bias** [7, 10, 40], which significantly impacts the current content ecosystem by reducing human creativity.

Alongside search engines, which serve as platforms for people to actively seek information, recommender systems also play a significant role as another important information system for information acquisition by users. They impact the daily life of humans through functions like news [23], product [38], and video [11] recommendations. Therefore, an important research question emerges: **RQ1: Whether source bias exist in recommender systems, as it has been identified in retrieval systems?** On the other hand, unlike the fixed query-document pairs in retrieval systems, in recommender systems, feedback data from the user interaction is reused to update the recommender system, forming a feedback loop involving users, data, and the recommender system as described in Figure 1. With the continuous increase in AIGC, they will gradually influence various stages of the feedback loop, raising another research question: **RQ2: In the LLMs era, whether the feedback loop process amplifies the phenomenon of source bias?**

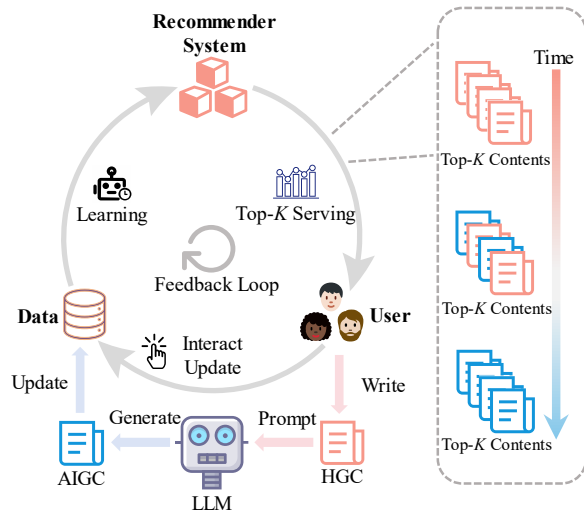


Figure 1: Source bias grows over time with the feedback loop of human, data, and the recommender system. The red color is used for HGC icon and the blue color is used for AIGC icon. The subsequent figures use the same color scheme.

To explore the aforementioned research questions, we first discuss the influx of AIGC into the content ecosystem of recommender systems across three phases: HGC dominate phase, HGC-AIGC coexist phase, and AIGC dominate phase as shown in Figure 2. These phases respectively correspond to the past, present, and future, representing the influence of different stages of AIGC flooding on recommender systems. Initially, in the HGC dominate phase, the influx of AIGC begins to pollute the candidate item set and influences the Top-K serving within the feedback loop, potentially introducing source bias. Subsequently, during the HGC-AIGC coexist phase, AIGC further taints users’ historical sequences via their interactions, which could amplify the existing source bias. Ultimately, in the AIGC dominate phase, the data tainted by AIGC predominates and is used to train the recommendation models, likely exacerbating source bias to significant levels.

To answer RQ1, we first construct evaluation datasets from three different domains by instructing LLMs to rewrite the provided text and obtain the AIGC copy. Then we evaluate several popular recommendation models using mixed candidate sets of HGC and AIGC items during **HGC dominate phase**. Our findings reveal that these models tend to rank AIGC at a higher position, uncovering that source bias is also prevalent in recommender systems.

For RQ2, we further conduct experiments by incorporating AIGC into users’ interaction history during the **HGC-AIGC coexist phase** and into the training data of recommendation models during the **AIGC dominate phase** in a feedback loop scenario. The results demonstrate that both users’ interaction behavior and the model’s updating process on polluted data will amplify the source bias. Finally, we can conclude that the source bias will continue to grow as the feedback loop progresses.

Furthermore, in the feedback loop scenario, our experimental results employing previously proposed debiasing methods [7, 10, 40] have shown that source bias not only persists but is also amplified

through the loop. Therefore, it is necessary to disrupt the propagation of source bias in the feedback loop mechanism, which raises a new research question: **RQ3: How can bias be maintained within a stable and controllable range in the feedback loop?** In response to RQ3, we introduce a novel debiasing method aimed at preventing the escalation the amplification of source bias during the influx of AIGC in the feedback loop. Specifically, our method first instructs LLMs to uniformly rewrite all training data, without the need to distinguish between HGC and AIGC. We then apply an L1 loss to constrain the outputs of the item encoder and the history encoder, ensuring that both HGC and AIGC, when sharing similar semantics, are mapped to corresponding embedding representations. Experimental results demonstrate that our method can effectively stabilize bias within acceptable limits and maintain the neutrality of model prediction across varying AIGC proportions.

The major contributions of this paper are summarized as follows:

- (1) We first validate the phenomenon of source bias in the recommender system, which is another important information system besides search engines.
- (2) We uncover that source bias amplifies as the user feedback progresses and the model’s training in a feedback loop scenario, further emphasizing the urgency of addressing source bias.
- (3) We propose a debiasing method that can effectively alleviate source bias during the feedback loop without the need to know the data source, thereby balancing the content ecosystem.

2 RELATED WORK

Large Language Models for Recommender Systems. Recent advancements in LLMs have attracted considerable interest among researchers to leverage these models [12, 21, 22, 36] to develop an enhanced recommender system. Some works utilize LLMs to generate knowledge-rich texts or use LLM-derived embeddings to enhance recommender systems, known as LLM-enhanced recommender systems [26, 34, 37]. Another line of work leverages LLMs that act as the ranking model to approach recommendation tasks, known as LLM-as-recommenders [3, 8, 14]. In addition to exploring how recommender systems can benefit from LLMs, we also need to consider the potential challenges that the development of LLMs may pose to recommender systems [9]. This paper primarily investigates the impact of AIGC on recommender systems, specifically focusing on the changes and influences of source bias in the feedback loop of recommender systems. luences of source bias in the feedback loop of recommender systems.

Effects of Artificial Intelligence Generated Content. The development of LLMs has propelled the prosperity of AIGC on the internet and bring about comprehensive impacts on society and technology [5, 9, 35]. Such vast amounts of AIGC can lead to a series of issues, such as the potential presence of misinformation [6, 39] or the generation of damaging content [15]. In addition to the impact on the content ecosystem, some recent studies have found that using AIGC to train AI models could lead to the collapse of next-generation models [2, 4, 28]. These issues in AIGC have attracted widespread attention and research efforts. Some recent studies indicate that neural retrieval models favor AIGC and will rank them higher in text and image retrieval systems. This phenomenon is

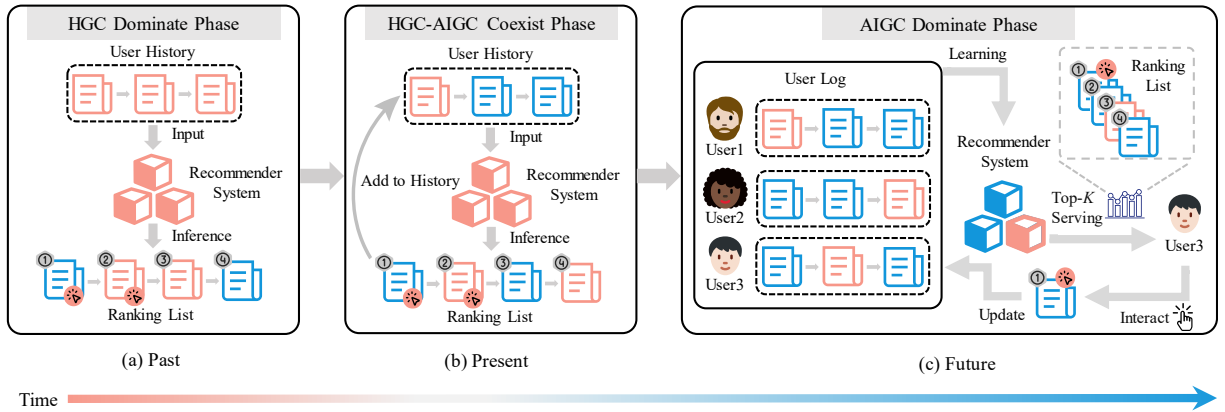


Figure 2: Three phases occur during the integration of AIGC into the recommendation content ecosystem: HGC dominate phase, HGC-AIGC coexist phase, and AIGC dominate phase. (1) The HGC dominate phase is a past period when AIGC has just flooded into the recommender systems and only influence the candidate list. (2) The HGC-AIGC coexist phase is a present period where the recommendation model’s inputs s contain an increasing number of AIGC. (3) The AIGC dominate phase is a future period during which AIGC influences each stage of the feedback loop.

referred to as source bias [7, 10, 40]. Our study examines the influence of source bias in another crucial information system, where AIGC influences model recommendations, users’ interaction, and model training in a typical feedback loop.

3 PRELIMINARIES

In this section, we formulate the recommendation problem, introduce three stages of AIGC flooding into recommender systems, and explore the role of the feedback loop in propagating source bias.

3.1 Problem Formulation

Assume that we have a set of items \mathcal{I} and a set of user interaction sequences \mathcal{S} , where $i \in \mathcal{I}$ denotes an item and $s \in \mathcal{S}$ denotes an interaction sequence. The numbers of items and sequences are denoted as $|\mathcal{I}|$ and $|\mathcal{S}|$, respectively. Generally, the interaction sequence s is chronologically ordered with items: $\{i_1, \dots, i_n\}$, where n is the number of interactions and i_t is the t -th item with which the user has interacted. For convenience, we use s_t to denote the subsequence, *i.e.*, $s_t = \{i_1, \dots, i_t\}$, where $1 \leq t < n$.

Based on the above notations, we now define the task of recommendation. Formally, given the history interaction sequence of a user $s_t = \{i_1, \dots, i_t\}$, the goal of recommendation is to train a recommendation model f_θ parameterized by θ . The model f_θ is used to predict the next item i_{t+1} the user is likely to interact with at the $(t + 1)$ -th step.

3.2 Three Phases of Recommendation Content

After AIGC integrates into the content ecosystem of recommender systems, it will gradually impact the three processes of the feedback loop over time: Top- K serving, users’ interaction, and model training. We divide the impact of AIGC on recommender systems by feedback loop over time into three phases: HGC Dominate, HGC-AIGC Coexist, and AIGC Dominate. Each phase corresponds to a real-world scenario representing the past, present, and future.

HGC Dominate Phase: With the widespread use of LLMs and

the popularization of AIGC on the internet, it is easy for HGC to have corresponding AIGC copies or even be directly generated by LLMs. Thus, the items selected for the recommendation model’s Top- K ranking are a combination of HGC and AIGC. In the HGC dominate phase, the research question aims to validate whether the recommendation models will rank AIGC at a higher position, a phenomenon known as source bias [7, 10, 40].

HGC-AIGC Coexist Phase: With the increasing proliferation of LLMs and AIGC on the Internet, the presence of AIGC in users’ recommendation candidate lists will rapidly grow. These contents will be interacted with users and added to their interaction sequences, which will be used as input for recommendation models later. In the HGC-AIGC coexist phase, the research question is whether source bias will be amplified when AIGC interacted with users’ interaction sequence.

AIGC Dominate Phase: In the future, with the decreasing cost and increasing accessibility of LLMs, AIGC will dominate the ecosystem of recommender systems. Furthermore, AIGC will influence any stage of the feedback loop, namely Top- K serving, users’ interaction, and model training in Figure 1. In other words, AIGC will pollute candidate list \mathcal{I} , users’ interaction history sequence s , and the model’s training data \mathcal{S} . Furthermore, within the iterative feedback loop, recommendation models undergo training on data \mathcal{S} that has been contaminated by AIGC. In the AIGC dominate phase, the research question is whether source bias will be amplified when recommendation models are trained on data polluted by AIGC.

In conclusion, the integration of AIGC into the recommender system will impact various aspects, such as the candidate item set, users’ interactions, and data used for model training in the feedback loop. Based on the affected aspects, the evolution of the recommender system will exhibit three phases: HGC Dominate, HGC-AIGC Coexist, and AIGC Dominate. We will explore the changes in source bias across these three phases to answer RQ1 and RQ2.

4 SOURCE BIAS IN RECOMMENDER SYSTEMS

In this section, we first introduce the experimental settings in Section 4.1 and then provide the data construction process and verify the AIGC quality through human evaluation in Section 4.2. In Section 4.3, we validate the existence of source bias in recommender systems during the HGC dominate phase. In Section 4.4 and Section 4.5, we verify that source bias is amplified in the feedback loop due to users' interaction behavior and the model training process.

4.1 Experimental Settings

4.1.1 Datasets. Our training and evaluation are conducted on a series of real-world datasets (Amazon [25]), comprising large corpora of product reviews and descriptions obtained from Amazon.com. Top-level product categories are treated as separate datasets, and we focus on three categories: "Health", "Beauty", and "Sports". We use the textual descriptions of products that users have commented on as input to predict which product the user might review next. Due to the low quality of short text rewriting¹, we exclude items with descriptions containing fewer than 20 words from the training set to maintain training stability.

We sort the data based on the review time of the target item and split it into training and testing sets in a 7:3 ratio. In the training dataset, we exclude users and items with fewer than five interactions and randomly select 4 negative items from the entire set for each product reviewed by users.

4.1.2 Recommendation Models. For our experiments, we select four representative models: BERT4Rec [29], SASRec [18], GRU4Rec [13], and LRURec [42]. **BERT4Rec:** It is a sequential recommendation model based on a bidirectional transformer encoder architecture, which is learned via predicting a masked item. **SASRec:** It is the first unidirectional transformer-based sequential recommender that leverages unidirectional self-attention to capture user-item transition patterns. **GRU4Rec:** It is a GRU-based encoder architecture for sequential recommendation that models user-item interactions. **LRURec:** It is a novel sequential recommendation model that efficiently captures user transition patterns through linear recurrence with matrix diagonalization. These models are enhanced by various pre-trained language models, including BERT [19] and RoBERTa [24]. We use the bert-base-uncased checkpoint for BERT and the roberta-base checkpoint for RoBERTa.

4.1.3 Evaluation Metrics. To evaluate the ranking performance of the recommendation model, we compute the Top- K Normalized Discounted Cumulative Gain (NDCG@ K) and Mean Average Precision (MAP@ K) separately for HGC and AIGC items, where $K \in \{3, 5\}$. To further measure the recommendation models' preferences for different source texts, the candidates during testing are divided into two parts: one part consists of original HGC, and the other part consists of copies of AIGC. To get a simple and efficient measuring way, we utilize the relative percentage difference [7, 10, 40]:

$$\text{Relative } \Delta = \frac{\text{Metric}_{\text{HGC}} - \text{Metric}_{\text{AIGC}}}{(\text{Metric}_{\text{HGC}} + \text{Metric}_{\text{AIGC}})/2} \times 100\%, \quad (1)$$

where $\text{Metric}_{\text{HGC}}$ and $\text{Metric}_{\text{AIGC}}$ are calculated on the same candidate set comprising both HGC and AIGC. For a given metric

¹LLM frequently expands short texts during the rewriting process.

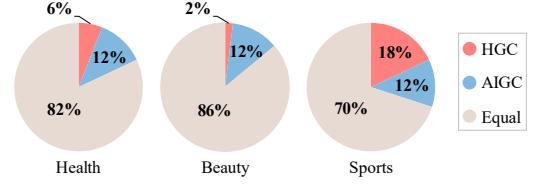


Figure 3: Quality verification of the constructed datasets through human evaluation.

(either NDCG@ K or MAP@ K), when measuring the metric for one data source, we set the labels of the other data source to 0. Relative $\Delta > 0$ indicates a preference of the recommendation models towards HGC, while Relative $\Delta < 0$ indicates a preference towards AIGC. The greater the absolute value of Relative Δ , the stronger the preference recommendation model for AIGC.

4.1.4 Experimental Details. To ensure computational efficiency, all pre-trained language models are frozen. All recommendation models are trained for 5 epochs, and the best-performing model on the development set is selected for testing on the test set. The batch size is set to 128, the learning rate is set to $1e-3$, and the Adam optimizer is used for training. The dimension of item vectors is set to 768, and all score calculations utilize the dot function. The text input to the model is truncated to 100 tokens, and the user's historical sequence is limited to 10 interactions. To ensure reproducibility, we run each experiment with five different seeds and report the averaged results.

4.2 AIGC Data Construction and Verification

4.2.1 Data Construction. Following the setting in previous works [7, 10, 40], we reconstruct the dataset from Amazon to evaluate source bias in recommender systems. For each item $i \in \mathcal{I}$, we utilize the same rewriting prompt "Please rewrite the following text: $\{\{human-written\}\}$ " to empower LLMs to produce text without extra constraints, all the while upholding semantic equivalence to the initial HGC. Specifically, we chose some popular LLMs ChatGPT (i.e., gpt-3.5-turbo-0613), Llama2 (i.e., llama-2-7b-chat) [32], Mistral (i.e., Mistral-7B-Instruct-v0.2) [17], and Gemini-pro (i.e., Gemini 1.5 Pro) [31] to rewrite each seed HGC, as these LLMs are the most widely used. The temperature of all LLMs for generation is set at 0.2 and the maximum generation length is 256.

After rewriting, we can obtain HGC data and the corresponding AIGC data for each dataset. Formally, we have two sets of items denoted by \mathcal{I}^H and \mathcal{I}^G , respectively. Here, $i^H \in \mathcal{I}^H$ represents an item written by a human, while $i^G \in \mathcal{I}^G$ represents an item generated by LLMs. Each item i^H has its corresponding AIGC copy $i^G \in \mathcal{I}^G$. In the LLMs era, the task of recommendation is to predict the next item i_{t+1} the user is likely to interact with from a mixed set of items $\mathcal{I} = \mathcal{I}^H \cup \mathcal{I}^G$, rather than just \mathcal{I}^H .

4.2.2 Human Evaluation. To validate that the rewritten data does not affect users' interaction behaviors, we conduct a human evaluation study by sampling 50 triples from the Health, Beauty, and Sports, respectively. For each domain, we recruit three colleagues for data annotation. Each human annotator is asked to indicate which item they would be more inclined to purchase based on the

Table 1: Performance comparison of recommendation models based on BERT and RoBERTa as text encoders for mixed HGC and AIGC item sets on the Health, Beauty, and Sports dataset. **Relative $\Delta < 0$ indicates that the recommendation models rank AIGC higher than HGC, while **Relative $\Delta > 0$** indicates that the recommendation models rank HGC higher than AIGC. The absolute value of Relative Δ indicates the degree of bias. The greater the absolute value of Relative Δ , the stronger the bias.**

PLM	Model	Corpus	Health				Beauty				Sports			
			NDCG@3	NDCG@5	MAP@3	MAP@5	NDCG@3	NDCG@5	MAP@3	MAP@5	NDCG@3	NDCG@5	MAP@3	MAP@5
BERT	BERT4Rec	Human-Written	26.49	35.22	22.88	27.70	21.53	30.31	18.42	23.27	26.00	35.54	22.06	27.37
		LLM-Generated	32.89	40.97	28.67	33.12	35.51	43.52	31.25	35.67	40.46	49.12	36.17	40.95
		Relative Δ	-21.57	-15.09	-22.47	-17.85	-49.00	-35.81	-51.66	-42.09	-43.49	-32.06	-48.46	-39.77
	SASRec	Human-Written	24.47	32.74	20.54	25.11	23.80	32.27	20.32	25.00	25.45	34.91	21.39	26.62
		LLM-Generated	39.82	47.60	35.80	40.10	34.51	43.38	30.28	35.18	44.56	52.73	39.95	44.48
		Relative Δ	-47.76	-36.99	-54.16	-45.96	-36.73	-29.38	-39.34	-33.85	-54.58	-40.68	-60.50	-50.24
	GRU4Rec	Human-Written	32.77	41.18	28.39	33.06	27.92	36.88	23.80	28.79	31.80	41.12	26.75	31.97
		LLM-Generated	41.28	48.74	36.92	41.03	44.21	52.41	39.54	44.09	51.73	58.92	47.03	51.00
		Relative Δ	-22.99	-16.80	-26.13	-21.51	-45.18	-34.78	-49.71	-42.01	-47.74	-35.60	-54.98	-45.87
	LRURec	Human-Written	34.22	42.13	30.13	34.51	31.30	39.26	27.26	31.66	34.12	42.31	29.55	34.09
		LLM-Generated	32.29	40.22	28.33	32.69	38.30	46.24	33.84	38.24	40.84	49.40	36.10	40.86
		Relative Δ	-20.13	5.80	4.65	6.16	5.43	-16.35	-21.54	-18.82	-17.92	-15.46	-19.93	-18.05
RoBERTa	BERT4Rec	Human-Written	29.37	37.60	25.40	29.97	26.29	34.86	22.84	27.59	31.14	39.98	27.15	32.05
		LLM-Generated	40.02	47.20	35.55	39.52	29.95	38.28	25.81	30.40	39.26	47.96	34.60	39.45
		Relative Δ	-30.68	-22.65	-33.30	-27.48	-13.02	-9.35	-12.22	-9.68	-23.06	-18.14	-24.16	-20.68
	SASRec	Human-Written	24.54	32.53	20.81	25.25	20.74	29.56	17.74	22.59	17.79	24.70	15.11	19.12
		LLM-Generated	38.63	46.76	34.32	38.78	27.87	36.93	24.24	29.26	26.57	35.65	23.00	28.00
		Relative Δ	-44.62	-35.91	-49.02	-42.26	-29.32	-22.17	-30.94	-25.70	-39.57	-36.30	-40.15	-37.69
	GRU4Rec	Human-Written	30.96	39.01	26.52	31.01	36.64	45.07	32.35	36.98	40.54	48.72	35.88	40.43
		LLM-Generated	44.10	50.98	39.48	43.26	34.61	43.58	30.00	34.98	43.43	50.82	38.61	42.72
		Relative Δ	-35.01	-26.60	-39.27	-32.97	5.69	3.36	7.55	5.55	-6.88	-4.20	-7.33	-5.51
	LRURec	Human-Written	25.35	34.33	21.19	26.15	33.06	40.23	29.40	33.36	30.24	39.49	26.30	31.42
		LLM-Generated	44.21	51.24	39.71	43.59	30.37	39.95	25.95	31.26	39.32	48.00	34.55	39.36
		Relative Δ	-54.21	-39.51	-60.80	-50.01	8.46	0.70	12.46	6.50	-26.11	-19.47	-27.12	-22.44

Table 2: Performance comparison (Relative Δ on NDCG@5) of recommendation models for mixed HGC and AIGC item sets on the Health, Beauty, and Sports dataset with AIGC copies generated by ChatGPT, Llama2, Mistral, and Gemini-Pro.

PLM	Model	Health				Beauty				Sports			
		ChatGPT	Llama2	Mistral	Gemini-Pro	ChatGPT	Llama2	Mistral	Gemini-Pro	ChatGPT	Llama2	Mistral	Gemini-Pro
BERT	BERT4Rec	-15.09	-	-9.093	-22.69	-35.81	-23.94	-18.75	-35.93	-32.06	-2.134	-38.23	-46.35
	SASRec	-36.99	-	-46.07	-50.66	-29.38	-36.57	-30.82	-62.06	-40.68	-31.7	-53.36	-56.17
	LRURec	-16.80	-	-18.3	-23.7	-34.78	-37.91	-33.83	-47.62	-35.60	-24.14	-49.58	-43.23
	LRURec	4.65	-	-10.83	-11.70	-16.35	-27.11	-13.32	-31.57	-15.46	-44.10	-35.7	-36.12
RoBERTa	BERT4Rec	-22.65	-	-27.44	-40.10	-9.35	-44.29	-20.79	-52.88	-18.14	-18.79	-30.30	-41.18
	SASRec	-35.91	-	-41.5	-52.13	-22.17	-42.13	-12.58	-25.95	-36.30	-81.06	-58.85	-54.86
	GRU4Rec	-26.60	-	-20.21	-27.27	3.36	-28.39	-16.50	-35.77	-4.20	-2.685	-19.71	-19.32
	LRURec	-39.51	-	-41.66	-49.38	0.70	-13.73	-7.91	-23.23	-19.47	-32.55	-39.02	-37.94

Note: We omit the result for Health dataset as Llama2 refuses to rewrite 97.7% of the product description due to that Health contains sensitive information.

textual description of products in the browsing purchase history, with options being “Human items”, “LLM items” and “Equal”. Each triple is annotated by at least three annotators, and the votes determine the final label. The evaluation results in Figure 3 demonstrate the consistency of humans’ interaction behaviors on HGC and AIGC, providing reliable assurance for the evaluation and analysis of source bias. The results further indicate that rewriting does not lead to quality improvement from a human perspective.

4.3 Source Bias in HGC Dominate Phase

In this subsection, we examine the recommendation model during the HGC dominate phase, aiming to explore whether the recommender system exhibits the phenomenon of source bias. We train recommendation models on each dataset with items from \mathcal{I}^H and test the model’s performance on candidate items from $\mathcal{I}^H \cup \mathcal{I}^G$. As shown in Table 1, it can be observed that most recommendation

models exhibit a preference for AIGC in terms of metrics such as NDCG@K and MAP@K, which is consistent with previous studies [7, 10, 40]. This phenomenon may stem from the shared semantic representation between LLMs and PLM models, enabling PLM models to better extract specific semantic information from AIGC. This specific semantic information can lead to a bias in semantic matching for recommendation models.

To verify the widespread presence of source bias in recommender systems, we test recommendation models on AIGC generated by popular LLMs such as ChatGPT, Llama2, Mistral, and Gemini-Pro. The results in Table 2 indicate the varying degrees of source bias on AIGC generated by different LLMs, confirming the prevalence and significance of source bias. Referring to a recent work [16], neural networks, trained with various objectives on diverse datasets are converging towards a common statistical model of reality within their representation spaces. This phenomenon further validates that

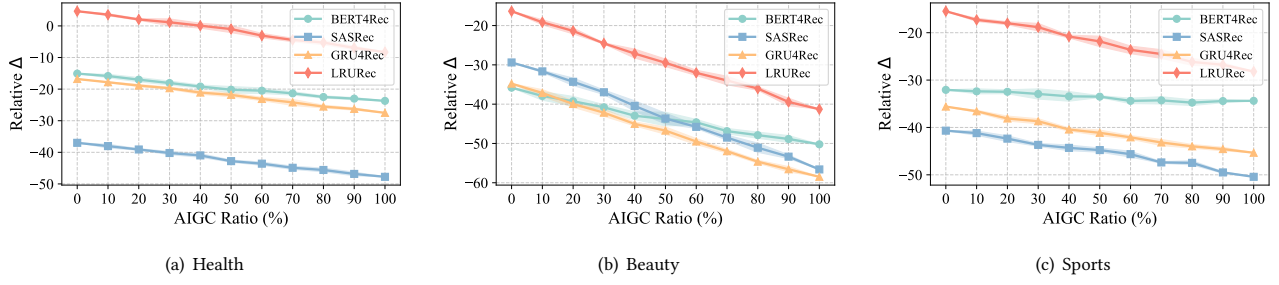


Figure 4: Relative Δ of recommendation models based on BERT as a text encoder for mixed HGC and AIGC item sets on the Health, Beauty, and Sports dataset, with AIGC copy generated by ChatGPT, is depicted along with its 95% confidence interval, shown with error bars. X-axis represents the ratio of AIGC in users' interaction sequence. If not specifically stated, in the following experiments, we will utilize ChatGPT to generate AIGC, using BERT as the encoder model, and Relative Δ is calculated based on NDCG@5.

LLMs may exhibit the same semantic representations as PLM models, even when using different data, structures, and optimization objectives. Furthermore, ChatGPT demonstrates a smaller source bias compared to other LLMs, likely due to its better alignment with human behavior during pre-training.

Finding 1: During the HGC dominate phase, various recommendation models based on different PLMs tend to show a preference for AIGC generated by various LLMs across three datasets from diverse domains.

4.4 Source Bias in HGC-AIGC Coexist Phase

In this subsection, we validate the recommendation models during the HGC-AIGC coexist phase, which aims to explore whether source bias will be amplified with the number of users' interaction on AIGC. When AIGC is further integrated into the recommender systems, users will interact with both HGC and AIGC. These items will be added to users' interaction history sequences, influencing the output of the recommendation model. In order to simulate this process, we train recommendation models on each dataset using items from \mathcal{I}^H . When testing, we vary the proportion of AIGC in users' interaction history sequence $s = \{i_1, \dots, i_n\}$. For $i_t \in s$, it originates from \mathcal{I}^H with probability p and from \mathcal{I}^G with probability $1 - p$ where p ranges from 0 to 1 in intervals of 0.1. This allows us to simulate the impact of users' interactions on AIGC on the source bias at different levels of AIGC propagation. The experimental results, as shown in Figure 4, indicate that the preference for AIGC of all sequential recommendation models increases as the proportion of AIGC in the historical sequence increases across the three datasets. While the extent of source bias exhibited by the same model varies across different datasets, they all show the same trend: the more AIGC the user interact with, the more pronounced the source bias phenomenon becomes in recommender systems, indicating a greater preference for AIGC by the models. Specifically, although the LRURec model initially exhibits a preference for HGC on Health, it gradually shows an increasing preference for AIGC in the history sequence increased.

Finding 2: In the feedback loop, the more users interact with AIGC, the model will recommend more AIGC in Top-K serving, thereby amplifying source bias.

4.5 Source Bias in AIGC Dominate Phase

In this subsection, we validate the recommendation models during the AIGC dominate phase, which aims to explore whether source bias will be further amplified with AIGC items participating in model training with the feedback loop. When AIGC dominates the recommender ecosystem in the future, it will influence any stage of the feedback loop, namely Top-K serving, interaction, and training as shown in Figure 1, corresponding to the candidate list \mathcal{I} , users' interaction history sequence s , and the model's training data \mathcal{S} . To investigate the changing trend of source bias during the AIGC dominate phase, we will construct a realistic scenario involving users' interactions. In this scenario, users are more inclined to interact with items positioned higher in the feedback loop for model training and testing rather than merely mixing the data proportions.

In the feedback loop, we will first train recommendation models with items from \mathcal{I}^H and use the trained models to simulate users' interactions on item sets $\mathcal{I}^H \cup \mathcal{I}^G$. To simulate users' behavior, the position-based click model (PBM) [1, 27] is used, where an interaction is registered only when the item is viewed and is relevant. Here, $E = 1$ indicates that an item is examined by a user. For each impression, the likelihood of examination is determined by the position in the list of candidate item [44]:

$$P(E = 1 | \text{rank}(i) = k) = \left(\frac{1}{k}\right)^\eta, \quad (2)$$

where η represents the hyper-parameter that controls the severity of position bias, and $\text{rank}(i)$ is the rank position of item i in the candidate item list. After obtaining users' interaction results, we use the proportion of users' interactions with AIGC to adjust the proportion of AIGC items in the interaction sequence s , as mentioned in Section 4.4, and then retrain the model using the aforementioned simulated interaction results and the mixed historical sequence. The specific training details can be found in the Appendix A. For

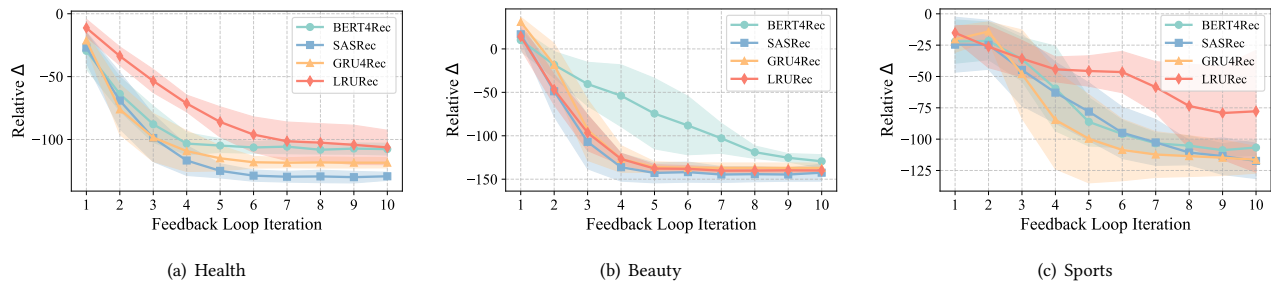


Figure 5: Performance comparison of recommendation models for mixed HGC and AIGC item sets on the Health, Beauty, and Sports dataset in different feedback loop iterations (X-axis), along with their 95% confidence intervals shown with error bars.

the training process described above, we iterate 10 iterations and assess the level of source bias in each model tested at each iteration. During testing, the proportion of AIGC in users’ interaction history is the same as the proportion of interactions with AIGC during training in that iteration.

To validate the rationality of the feedback loop environment and test how source bias changes under different position bias conditions, we set different values for η and observe the source bias of the model after 10 iterations of loop training. The results are shown in Table 3. It can be observed that regardless of the value of η , the source bias still exists after the feedback loop. Moreover, as the value of η increases, the source bias becomes more severe at the end of the feedback loop. If users have a stronger position bias when interacting, the AIGC in the higher position caused by source bias will be interacted at a higher probability, which will lead to more AIGC in the training data. Finally, the source bias will propagate more rapidly in the feedback loop. In the subsequent experiments, we set η to $+\infty$, indicating that users will interact with the positive samples at the top positions than others.

In addition, under the condition of $\eta = +\infty$, we also test the source bias phenomenon at different iterations of the feedback loop. The results are shown in Figure 5. We can see that the bias of all models increases with each iteration until it converges to a value near the end. During this process, source bias plays a role within the feedback loop and is thereby amplified. It is worth noting that in Beauty, the models do not initially exhibit source bias. However, it still emerges and amplifies as the feedback loop progresses, further indicating the ubiquity of source bias even if the model initially does not show a preference for AIGC.

Finding 3: Finally, by introducing AIGC pollute the feedback loop, including Top- K serving, users’ interactions, and model training, the source bias will be pushed to the top.

Through a series of experiments, we have found that source bias exists in recommender systems and can be amplified by the feedback loop. As AIGC continues to proliferate, this bias may cause a range of issues. First, recommending is a passive behavior compared to actively searching in search scenarios. Therefore, the presence of source bias makes it more likely for users to interact

Table 3: Relative Δ of recommendation models trained in the feedback loop after 10 iterations, which is the average result on three datasets.. The results are the average value of five experiments, with the standard deviations in parentheses.

η	1	10	$+\infty$
BERT4Rec	-33.39(± 7.92)	-100.50 (± 4.41)	-106.60 (± 4.91)
SASRec	-25.11(± 4.93)	-126.90(± 7.10)	-128.40(± 3.29)
GRU4Rec	-2.96(± 14.60)	-117.50(± 8.71)	-120.00(± 3.07)
LRURec	-13.95(± 8.02)	-66.60(± 62.00)	-112.2(± 9.21)

with potentially harmful AIGC, as users may not have explicit intentions. Moreover, a significant amount of AIGC is integrated into the recommender system, which further amplifies the source bias phenomenon through the feedback loop. Over time, the interaction between AIGC and source bias will mutually reinforce each other, impacting the entire content creation ecosystem.

5 DEBIAS DURING THE FEEDBACK LOOP

In this section, we propose a debiasing method to eliminate source bias during the feedback loop and conduct several experiments to validate its effectiveness.

5.1 Motivation

In previous sections, we validate the presence of source bias in recommender systems. Furthermore, with the proliferation of AIGC on the internet, source bias amplifies throughout the feedback loop, thus accelerating the expansion of AIGC. Therefore, it is crucial to propose an effective debiasing method and maintain its effectiveness in dynamically changing feedback loop scenarios. In previous work, some effective methods [10, 40] to mitigate source bias have been suggested in document ranking and text-image retrieval tasks. However, these methods can not be directly applied to the dynamic feedback loop scenarios of recommender systems. **First**, these methods focus on debiasing document representations while overlooking context representations that are intertwined with AIGC and expand with the progression of the feedback loop. This expansion contributes to the amplification of source bias. **Second**, previous methods are white-box and therefore require knowledge of whether the text comes from HGC or AIGC, which is challenging

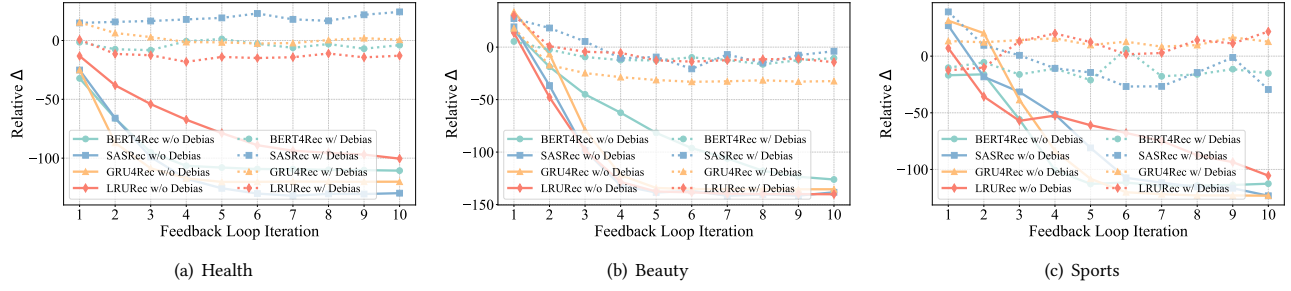


Figure 6: Relative Δ of recommendation models for mixed HGC and AIGC item sets on Health, Beauty, and Sports datasets in various feedback loop iterations (X-axis).

Table 4: Relative Δ of recommendation models trained with previous debiasing methods in the feedback loop after 10 iterations. The results are the averaged number of five experiments, with the standard deviations in parentheses.

Model	Health	Beauty	Sports
BERT4Rec	-100.68 (± 15.88)	-36.40 (± 113.83)	-111.90 (± 16.06)
SASRec	-130.91 (± 8.19)	-159.62 (± 2.65)	-141.20 (± 5.42)
GRU4Rec	-98.85 (± 48.20)	-147.38 (± 3.10)	-142.94 (± 3.37)
LRURec	-114.37 (± 16.67)	-157.62 (± 2.87)	-120.55 (± 30.99)

to achieve in the context of a feedback loop, even with text detection techniques. **Third**, these methods utilize hinge loss, which may cause the model to gradually favor HGC during the feedback loop process, leading to the development of new biases. Moreover, we employ the debiasing methods from previous studies to train the model in a feedback loop, and the results in Table 4 demonstrate the necessity of new methods in dynamic scenarios.

Considering the aforementioned problems, we propose our debiasing methods from three perspectives. **First**, we propose a debiasing constraint on both item representation and history representation. **Second**, a black-box strategy is used to enable the method to focus directly on the differences between the rewritten text before and after, without requiring knowledge of the source of the training text. **Third**, the hinge loss is replaced with the L1 loss to ensure the model does not favor either HGC or AIGC.

5.2 Debiasing Methods

For each i in I , regardless of whether it originates from I^H or I^G , its corresponding rewriting copy i' in I' is derived from the rewriting process of LLM as described in Section 4.2. In this way, we obtain the original training data triple (s_t, i_{t+1}, i'_{t+1}) for feedback loop training. We utilize the L1 loss function to calculate the difference in scores between i_{t+1} and i'_{t+1} as:

$$\mathcal{L}_{\text{Debias-I}} = \sum_{s \in S} \sum_{t=1}^{n-1} |f_{\theta}(s_t, i'_{t+1}) - f_{\theta}(s_t, i_{t+1})|, \quad (3)$$

which can eliminate the additional score introduced by the LLM rewriting process compared to the user interaction sequence s . Hence, it can be incorporated as a component of the loss function

Table 5: Performance of recommendation models on three datasets. “w/o Debias” means a model trained without our proposed debiasing method, while “w/ Debias” means a model trained with our proposed debiasing method.

Model	Health		Beauty		Sports	
	w/o Debias	Debias	w/o Debias	Debias	w/o Debias	Debias
BERT4Rec	63.82	63.28 -0.54	64.15	63.60 -0.55	62.20	60.55 -1.65
SASRec	64.72	65.76 +1.04	65.62	65.75 +0.13	64.37	63.34 -1.03
GRU4Rec	68.59	72.71 +4.12	68.44	71.61 +3.17	68.79	73.10 +4.32
LRURec	65.37	66.73 +1.36	66.59	68.31 +1.72	64.60	64.63 +0.03

to alleviate the source bias. What’s more, for each item i in the user interaction sequence s , we can obtain its rewritten copy s' by replacing each item i with corresponding i' . Again, we utilize the L1 loss function to calculate the difference in scores between s and s' in comparison to candidate item i . Furthermore, in addition to aligning the embedding representations of user interaction sequences s and s' before and after rewriting, we aim to maximize the entropy \mathbb{H} of the embedding representation for each interaction sequence s and s' . This ensures that the embedding representations $\text{Emb}(s)$ generated from different s composed of different items i move farther away from each other. The debiasing loss for the history encoder side can be expressed as follows:

$$\mathcal{L}_{\text{Debias-U}} = \sum_{s \in S} \sum_{t=1}^{n-1} |f_{\theta}(s'_t, i_{t+1}) - f_{\theta}(s_t, i_{t+1})| + \mathbb{H}(\text{Emb}(s'_t)) + \mathbb{H}(\text{Emb}(s_t)), \quad (4)$$

which can measure the additional score resulting from the history encoder’s preference for user interaction sequence s' combined with AIGC item, in comparison to item i . Therefore, this can also be used as part of the loss function to mitigate the source bias caused by the history encoder. Based on the additional constraints defined in Eq. (3) and Eq. (4), we can define the final loss for model training:

$$\mathcal{L} = \mathcal{L}_{\text{ranking}} + \alpha \mathcal{L}_{\text{Debias-I}} + \beta \mathcal{L}_{\text{Debias-U}}, \quad (5)$$

where $\mathcal{L}_{\text{ranking}}$ can be either contrastive loss or regression loss. α and β are the debiasing coefficients that can balance the recommendation performance and the level of the source bias. The larger coefficient indicates a greater penalty on the biased samples, which may result in a decrease in the recommendation performance.

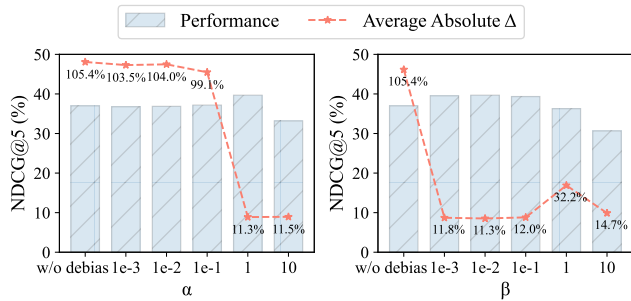


Figure 7: Performance and Average Absolute Δ of recommendation models on Health with different coefficients α and β in our proposed debiasing method.

5.3 Experimental Results

Figure 6 illustrates the Relative Δ of the model and the debiasing model at different iterations of the feedback loop. The dashed line represents the model with our proposed method. Compared to previous methods, our approach focuses solely on the differences before and after rewriting, which enables us to continuously achieve debiasing effects in iterative feedback, resulting in a smaller absolute Relative Δ . Furthermore, the dashed line remaining within a stable range also demonstrates that L1 loss can prevent the model from biasing towards either HGC or AIGC during the dynamic process.

Table 5 presents the ranking performance of models on all datasets. Our debiasing method not only eliminates biases but also enhances model performance in most cases. Suggested by these findings it can be found that introducing hard negative samples during the debiasing process of AIGC appears to enhance the model’s capacity to differentiate between similar items.

5.4 Further Analysis

5.4.1 Performance w.r.t. the Coefficients α and β . As described in Eq.(5), our proposed debiasing method incorporates coefficients α and β to balance the loss between ranking and debiasing on source bias, thereby achieving a trade-off between model performance and unbiasedness. In the experiment, we vary the debiasing coefficients α and β within the range of $\{1e-3, 1e-2, 1e-1, 1, 10\}$. When varying one coefficient, we keep the other coefficient at the value where the model performs best in terms of Average Absolute Δ , which is the average absolute value of the Relative Δ that the model exhibits during the feedback loop process. The original models trained without debiasing constraints are denoted as “w/o debias”.

The results of the Health dataset are presented in Figure 7. We can observe that as α increases, the model’s Average Absolute Δ gradually decreases and the model’s ability to mitigate bias is demonstrated by the application of debiasing constraints $\mathcal{L}_{\text{Debias-I}}$. Furthermore, as the model’s Average Absolute Δ decreases, it can maintain ranking performance and notably outperform the model without debiasing constraints. This phenomenon is likely due to the inclusion of AIGC samples, which may enhance the model’s ability to discern relevance among similar documents. At the same time, when α becomes extremely large, the model’s performance decreases, which could be attributed to that $\mathcal{L}_{\text{Debias-I}}$ causing the

Table 6: Average Absolute Δ of recommendation model on Health, Beauty and Sports datasets. “w/o Debias-U” means the model trained with debiasing constraints that not include $\mathcal{L}_{\text{Debias-U}}$ while “w/o Debias-I” means the model trained with debiasing constraints that not include $\mathcal{L}_{\text{Debias-I}}$.

Model	NDCG@5			MAP@5		
	Debias	w/o Debias-U	w/o Debias-I	Debias	w/o Debias-U	w/o Debias-I
BERT4Rec	8.18	8.65 +0.47	25.86 +17.68	8.28	9.84 +1.56	29.40 +19.56
SASRec	21.69	18.43 -3.26	124.80 +103.11	24.39	20.84 -3.55	135.84 +115.00
GRU4Rec	6.45	8.07 +1.62	130.00 +123.55	7.12	9.65 +2.53	142.89 +135.77
LRURec	8.97	29.72 +20.75	122.30 +113.33	11.34	32.74 +21.4	131.93 +120.59

model to overly prioritize distinguishing between HGC and AIGC instead of focusing on ranking candidate items. Similar phenomenon also occur when adjusting the β . Furthermore, when β becomes larger, the model’s performance decreases. This could be due to the fact that forcing different interaction sequences to be closer together could lead the model to learn similar representations, thereby disrupting the model’s ranking ability.

5.4.2 Ablation Study. In this experiment, we investigate whether the two proposed components of loss, $\mathcal{L}_{\text{Debias-U}}$ and $\mathcal{L}_{\text{Debias-I}}$, can effectively eliminate the source bias. We conduct experiments to evaluate the Average Absolute Δ on the models trained only on our debiasing method without $\mathcal{L}_{\text{Debias-U}}$ and $\mathcal{L}_{\text{Debias-I}}$, denoted as “w/o Debias-U” and “w/o Debias-I”, respectively. The results in Figure 6 show that the Average Absolute Δ of the model improves across all models. After removing all debiasing constraints except for the “w/o Debias-U model” with SASRec implementation, the Average Absolute Δ increases. This observation confirms the effectiveness of constraining the item encoder and user encoder in our proposed loss function. Meanwhile, the $\mathcal{L}_{\text{Debias-I}}$ loss is more effective compared to the $\mathcal{L}_{\text{Debias-U}}$ loss may result from the fact that debiasing directly on the items used for evaluation is more straightforward.

5.4.3 Visualize of Interaction Sequence Representation. As shown in Figure 8, we visualize the interaction sequence representation $\text{Emb}(s)$ of models with various debiasing constraints using T-SNE [33], in which the models are denoted as w/o $\mathbb{H}(\text{Emb}(s))$ and w/ $\mathbb{H}(\text{Emb}(s))$ to indicate whether the term maximizing user embedding entropy is included in $\mathcal{L}_{\text{Debias-U}}$. Both types of debiasing constraints on $\text{Emb}(s)$ can maintain the mapping representation of historical sequences before and after rewriting. However, our proposed debiasing constraints, which involve maximizing entropy \mathbb{H} in addition to minimizing the distances between s and s' , can make the distributions of various user history embeddings more uniform. This approach ensures that different historical sequences do not end up with the same representation, thus maintaining the model’s ranking performance while keeping the same representation for AIGC sequence and HGC sequence.

6 CONCLUSION

In this paper, we delve into exploring the source bias in recommender systems. Through extensive experiments with several representative recommendation models across three datasets from different domains, we uncover the prevalence of source bias in recommender systems. Furthermore, we validate that source bias

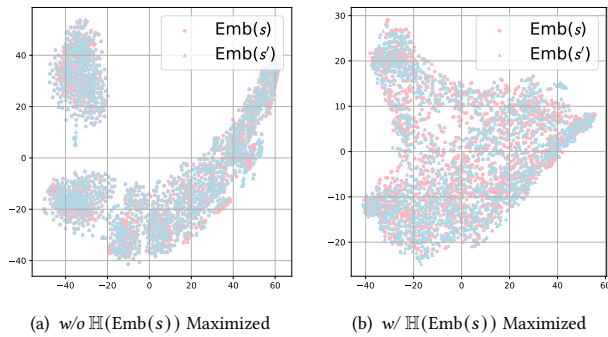


Figure 8: User history embedding visualization of GRU4Rec trained without and with $\mathbb{H}(\text{Emb}(s))$ on Health dataset.

is gradually amplified in the feedback loop, where AIGC will be incorporated into users' interaction histories and the training data as time progresses. To mitigate source bias and prevent its further amplification in the feedback loop, we propose a black-box debiasing solution that ensures the impartiality of the model prediction towards both HGC and AIGC in the feedback loop.

REFERENCES

- [1] Qingyao Ai, Tao Yang, Huazheng Wang, and Jiaxin Mao. 2021. Unbiased learning to rank: online or offline? *ACM Transactions on Information Systems (TOIS)* 39, 2 (2021), 1–29.
- [2] Sina Alemohammad, Josue Casco-Rodriguez, Lorenzo Luzi, Ahmed Imtiaz Humayun, Hossein Babaei, Daniel Lejeune, Ali Siahkoobi, and Richard G Baraniuk. 2023. Self-consuming generative models go mad. *arXiv preprint arXiv:2307.01850* (2023).
- [3] Keqin Bao, Jizhi Zhang, Yang Zhang, Wenjie Wang, Fuli Feng, and Xiangnan He. 2023. Tallrec: An effective and efficient tuning framework to align large language model with recommendation. In *Proceedings of the 17th ACM Conference on Recommender Systems*. 1007–1014.
- [4] Martin Briesch, Dominik Sobania, and Franz Rothlauf. 2023. Large Language Models Suffer From Their Own Output: An Analysis of the Self-Consuming Training Loop. *arXiv preprint arXiv:2311.16822* (2023).
- [5] Yihan Cao, Siyu Li, Yixin Liu, Zhiling Yan, Yutong Dai, Philip S Yu, and Lichao Sun. 2023. A comprehensive survey of ai-generated content (aigc): A history of generative ai from gan to chatgpt. *arXiv preprint arXiv:2303.04226* (2023).
- [6] Canyu Chen and Kai Shu. 2023. Combating misinformation in the age of llms: Opportunities and challenges. *arXiv preprint arXiv:2311.05656* (2023).
- [7] Sunhao Dai, Weihao Liu, Yuqi Zhou, Liang Pang, Rongju Ruan, Gang Wang, Zhenhua Dong, Jun Xu, and Ji-Rong Wen. 2024. Cocktail: A Comprehensive Information Retrieval Benchmark with LLM-Generated Documents Integration. *Findings of the Association for Computational Linguistics: ACL 2024* (2024).
- [8] Sunhao Dai, Ninglu Shao, Haiyuan Zhao, Weijie Yu, Zihua Si, Chen Xu, Zhongxiang Sun, Xiao Zhang, and Jun Xu. 2023. Uncovering chatgpt's capabilities in recommender systems. In *Proceedings of the 17th ACM Conference on Recommender Systems*. 1126–1132.
- [9] Sunhao Dai, Chen Xu, Shicheng Xu, Liang Pang, Zhenhua Dong, and Jun Xu. 2024. Unifying Bias and Unfairness in Information Retrieval: A Survey of Challenges and Opportunities with Large Language Models. *Proceedings of the 30th ACM SIGKDD Conference on Knowledge Discovery and Data Mining* (2024).
- [10] Sunhao Dai, Yuqi Zhou, Liang Pang, Weihao Liu, Xiaolin Hu, Yong Liu, Xiao Zhang, Gang Wang, and Jun Xu. 2024. Neural Retrievers are Biased Towards LLM-Generated Content. *Proceedings of the 30th ACM SIGKDD Conference on Knowledge Discovery and Data Mining* (2024).
- [11] James Davidson, Benjamin Liebald, Junning Liu, Palash Nandy, Taylor Van Vleet, Ullas Gargi, Sujoy Gupta, Yu He, Mike Lambert, Blake Livingston, et al. 2010. The YouTube video recommendation system. In *Proceedings of the fourth ACM conference on Recommender systems*. 293–296.
- [12] Wenqi Fan, Zihuai Zhao, Jiatong Li, Yunqing Liu, Xiaowei Mei, Yiqi Wang, Jiliang Tang, and Qing Li. 2023. Recommender systems in the era of large language models (llms). *arXiv preprint arXiv:2307.02046* (2023).
- [13] Balázs Hidasi, Alexandros Karatzoglou, Linas Baltrunas, and Domonkos Tikk. 2015. Session-based recommendations with recurrent neural networks. *arXiv preprint arXiv:1511.06939* (2015).
- [14] Yupeng Hou, Junjie Zhang, Zihan Lin, Hongyu Lu, Ruobing Xie, Julian McAuley, and Wayne Xin Zhao. 2024. Large language models are zero-shot rankers for recommender systems. In *European Conference on Information Retrieval*. Springer, 364–381.
- [15] Yangsibo Huang, Samyak Gupta, Mengzhou Xia, Kai Li, and Danqi Chen. 2023. Catastrophic Jailbreak of Open-source LLMs via Exploiting Generation. In *The Twelfth International Conference on Learning Representations*.
- [16] Minyoung Huh, Brian Cheung, Tongzhou Wang, and Phillip Isola. 2024. The Platonic Representation Hypothesis. *arXiv preprint arXiv:2405.07987* (2024).
- [17] Albert Q Jiang, Alexandre Sablayrolles, Arthur Mensch, Chris Bamford, Devendra Singh Chaplot, Diego de las Casas, Florian Bressand, Gianna Lengyel, Guillaume Lample, Lucile Saulnier, et al. 2023. Mistral 7B. *arXiv preprint arXiv:2310.06825* (2023).
- [18] Wang-Cheng Kang and Julian McAuley. 2018. Self-attentive sequential recommendation. In *2018 IEEE international conference on data mining (ICDM)*. IEEE, 197–206.
- [19] Jacob Devlin Ming-Wei Chang Kenton and Lee Kristina Toutanova. 2019. BERT: Pre-training of Deep Bidirectional Transformers for Language Understanding. In *Proceedings of NAACL-HLT*. 4171–4186.
- [20] Viet Lai, Nghia Ngo, Amir Pouran Ben Veysseh, Hiêu Mãn, Franck Dernoncourt, Trung Bui, and Thien Nguyen. 2023. ChatGPT Beyond English: Towards a Comprehensive Evaluation of Large Language Models in Multilingual Learning. In *Findings of the Association for Computational Linguistics: EMNLP 2023*. 13171–13189.
- [21] Yongqi Li, Xinyu Lin, Wenjie Wang, Fuli Feng, Liang Pang, Wenjie Li, Liqiang Nie, Xiangnan He, and Tat-Seng Chua. 2024. A Survey of Generative Search and Recommendation in the Era of Large Language Models. *arXiv preprint arXiv:2404.16924* (2024).
- [22] Jianghao Lin, Xinyi Dai, Yunjia Xi, Weiwen Liu, Bo Chen, Xiangyang Li, Chenxu Zhu, Huifeng Guo, Yong Yu, Ruiming Tang, et al. 2023. How can recommender systems benefit from large language models: A survey. *arXiv preprint arXiv:2306.05817* (2023).
- [23] Jiahui Liu, Peter Dolan, and Elin Rønby Pedersen. 2010. Personalized news recommendation based on click behavior. In *Proceedings of the 15th international conference on Intelligent user interfaces*. 31–40.
- [24] Yinhan Liu, Myle Ott, Naman Goyal, Jingfei Du, Mandar Joshi, Danqi Chen, Omer Levy, Mike Lewis, Luke Zettlemoyer, and Veselin Stoyanov. 2019. Roberta: A robustly optimized bert pretraining approach. *arXiv preprint arXiv:1907.11692* (2019).
- [25] Julian McAuley, Christopher Targett, Qinfeng Shi, and Anton Van Den Hengel. 2015. Image-based recommendations on styles and substitutes. In *Proceedings of the 38th international ACM SIGIR conference on research and development in information retrieval*. 43–52.
- [26] Xubin Ren, Wei Wei, Lianghao Xia, Lixin Su, Suqi Cheng, Junfeng Wang, Dawei Yin, and Chao Huang. 2023. Representation learning with large language models for recommendation. *arXiv preprint arXiv:2310.15950* (2023).
- [27] Matthew Richardson, Ewa Dominowska, and Robert Ragno. 2007. Predicting clicks: estimating the click-through rate for new ads. In *Proceedings of the 16th international conference on World Wide Web*. 521–530.
- [28] Ilya Shumailov, Zakhar Shumaylov, Yiren Zhao, Yarin Gal, Nicolas Papernot, and Ross Anderson. 2023. Model dementia: Generated data makes models forget. *arXiv e-prints* (2023), arXiv:2305.
- [29] Fei Sun, Jun Liu, Jian Wu, Changhua Pei, Xiao Lin, Wenwu Ou, and Peng Jiang. 2019. BERT4Rec: Sequential recommendation with bidirectional encoder representations from transformer. In *Proceedings of the 28th ACM international conference on information and knowledge management*. 1441–1450.
- [30] Yiming Tan, Dehai Min, Yu Li, Wenbo Li, Nan Hu, Yongrui Chen, and Guilin Qi. 2023. Evaluation of ChatGPT as a question answering system for answering complex questions. *arXiv preprint arXiv:2303.07992* (2023).
- [31] Gemini Team, Rohan Anil, Sebastian Borgeaud, Yonghui Wu, Jean-Baptiste Alayrac, Jiahui Yu, Radu Soricut, Johan Schalkwyk, Andrew M Dai, Anja Hauth, et al. 2023. Gemini: a family of highly capable multimodal models. *arXiv preprint arXiv:2312.11805* (2023).
- [32] Hugo Touvron, Louis Martin, Kevin Stone, Peter Albert, Amjad Almahairi, Yasmine Babaei, Nikolay Bashlykov, Soumya Batra, Prajwal Bhargava, Shruti Bhosale, et al. 2023. Llama 2: Open foundation and fine-tuned chat models. *arXiv preprint arXiv:2307.09288* (2023).
- [33] Laurens Van der Maaten and Geoffrey Hinton. 2008. Visualizing data using t-SNE. *Journal of machine learning research* 9, 11 (2008).
- [34] Wei Wei, Xubin Ren, Jiabin Tang, Qinyong Wang, Lixin Su, Suqi Cheng, Junfeng Wang, Dawei Yin, and Chao Huang. 2024. Llmrec: Large language models with graph augmentation for recommendation. In *Proceedings of the 17th ACM International Conference on Web Search and Data Mining*. 806–815.
- [35] Jiayang Wu, Wensheng Gan, Zefeng Chen, Shicheng Wan, and Hong Lin. 2023. Ai-generated content (aigc): A survey. *arXiv preprint arXiv:2304.06632* (2023).
- [36] Likang Wu, Zhi Zheng, Zhaopeng Qiu, Hao Wang, Hongchao Gu, Tingjia Shen,

- Chuan Qin, Chen Zhu, Hengshu Zhu, Qi Liu, et al. 2023. A survey on large language models for recommendation. *arXiv preprint arXiv:2305.19860* (2023).
- [37] Yunjia Xi, Weiwen Liu, Jianghao Lin, Jieming Zhu, Bo Chen, Ruiming Tang, Weinan Zhang, Rui Zhang, and Yong Yu. 2023. Towards open-world recommendation with knowledge augmentation from large language models. *arXiv preprint arXiv:2306.10933* (2023).
- [38] Bo Xiao and Izak Benbasat. 2007. E-commerce product recommendation agents: Use, characteristics, and impact. *MIS quarterly* (2007), 137–209.
- [39] Danni Xu, Shaojing Fan, and Mohan Kankanhalli. 2023. Combating misinformation in the era of generative AI models. In *Proceedings of the 31st ACM International Conference on Multimedia*. 9291–9298.
- [40] Shicheng Xu, Danyang Hou, Liang Pang, Jingcheng Deng, Jun Xu, Huawei Shen, and Xueqi Cheng. 2024. Invisible Relevance Bias: Text-Image Retrieval Models Prefer AI-Generated Images. *Proceedings of the 47th international ACM SIGIR conference on research and development in information retrieval* (2024).
- [41] Shicheng Xu, Liang Pang, Huawei Shen, Xueqi Cheng, and Tat-Seng Chua. 2024. Search-in-the-Chain: Interactively Enhancing Large Language Models with Search for Knowledge-intensive Tasks. In *Proceedings of the ACM on Web Conference 2024*. 1362–1373.
- [42] Zhenrui Yue, Yueqi Wang, Zhankui He, Huimin Zeng, Julian McAuley, and Dong Wang. 2024. Linear recurrent units for sequential recommendation. In *Proceedings of the 17th ACM International Conference on Web Search and Data Mining*. 930–938.
- [43] Haopeng Zhang and Xiao Liu. 2023. Extractive Summarization via ChatGPT for Faithful Summary Generation. In *Foundations and Applications in Large-scale AI Models Workshop at KDD 2023 conference (KDD LLM4AI'23), August 6-10, 2023, Long Beach, CA, USA*.
- [44] Haiyuan Zhao, Jun Xu, Xiao Zhang, Guohao Cai, Zhenhua Dong, and Ji-Rong Wen. 2023. Unbiased Top-k Learning to Rank with Causal Likelihood Decomposition. In *Proceedings of the Annual International ACM SIGIR Conference on Research and Development in Information Retrieval in the Asia Pacific Region*. 129–138.
- [45] Wayne Xin Zhao, Kun Zhou, Junyi Li, Tianyi Tang, Xiaolei Wang, Yupeng Hou, Yingqian Min, Beichen Zhang, Junjie Zhang, Zican Dong, et al. 2023. A survey of large language models. *arXiv preprint arXiv:2303.18223* (2023).

A APPENDIX: FEEDBACK LOOP TRAINING

Algorithm 1: Feedback Loop for Model Training

Input: Interaction dataset \mathcal{S} ; number of feedback loop iterations E ; parameters η, p

Output: Trained models $f_{\theta}^1, f_{\theta}^2, \dots, f_{\theta}^E$

```

1  $p \leftarrow 0$ 
2  $\mathcal{S}^e \leftarrow \mathcal{S}$ 
3 for  $e = 1, \dots, E$  do
4   Train model  $f_{\theta}^e$  on dataset  $\mathcal{S}^e$ 
5    $\mathcal{S}^e \leftarrow \{\}$ 
6   for  $(s_t, i_{t+1})$  in  $\mathcal{S}$  do
7      $s_t \leftarrow \{i^L \mathbb{1}(\text{Bernoulli}(p^{e-1}) = 1) + i^H \mathbb{1}(\text{Bernoulli}(p^{e-1}) \neq 1) : i \in s_t\}$ 
8     Get users' interaction probabilities  $\mathcal{Y}$  with Eq. ((2))
9     Sample users' interaction item  $i_{t+1}$  from  $\mathcal{I}$  with  $\mathcal{Y}$ 
10     $\mathcal{S}^e \leftarrow \mathcal{S}^e \cup (s_t, i_{t+1})$ 
11  end
12  Update  $p$  with probability of  $i_{t+1}$  from  $\mathcal{I}^G$ 
13 end
14 return  $f_{\theta}^1, f_{\theta}^2, \dots, f_{\theta}^E$ 

```

Specifically, we have a dataset \mathcal{S} consisting of triples (s_t, i_{t+1}) , where s_t represents the interaction sequence and i_{t+1} represents the item interacted by human from \mathcal{I}^H in the next time given s_t . We use the dataset \mathcal{S} for training and employ the trained model f_{θ} for simulating users' interactions. First, we vary the proportion of AIGC in users' interaction history sequences s as shown in Line 7. Then, we utilize the mixed interaction history sequence s as input to calculate users' interaction probabilities with f_{θ} , as shown in Line 8. Based on the probabilities, we sample the item i_{t+1} the user may likely to interact with from the entire set \mathcal{I} . This implies that the user may interact with i_{t+1}^H or the corresponding AIGC copy i_{t+1}^G as illustrated in Line 9. Finally, we will update the simulation behavior triplet with new training data \mathcal{S}^e , as shown in Line 10. After completing the simulation, we will update the probability of the user interaction with AIGC as demonstrated in the Line 12 and begin the next iteration of feedback loop training. To simulate a real scenario and ensure comparability of results, we divide \mathcal{S} equally into two parts and alternate feedback loop training between them. We only select models trained on the first part for testing.

B APPENDIX: DATASET DETAILS

The statistics of the experimental datasets after processing are shown in Figure 7.

Table 7: Statistics of the experimental datasets.

Dataset	Health	Beauty	Sports
# Users	18,036	11,391	16,639
# Items	13,972	11,897	13,089
# Interaction Behaviors	346,355	198,502	296,337

We provide examples of HGC and the corresponding AIGC by ChatGPT, Llama2, Mistral, and Gemini-Pro on Health, Beauty and Sports dataset, as shown in Figure 8, Figure 9, and Figure 10, respectively.

Table 8: Examples of HGC and AIGC on Health dataset.

Human
Contains the botanicals sage & lemongrass for effectively fighting odor & aloe vera to soothe the skin. Gentle, effective, natural. Mild formula for reliable odor protection. Our natural deodorant combines the botanicals sage and lemongrass, in a formula that is effective at fighting odor, yet gentle on the skin. The fragrance has been selected for its pleasant scent, as well as for its mildness, and we never use artificial preservatives, colors, or harsh alcohol. No animal ingredients. No animal testing. No artificial ingredients.

ChatGPT
Our gentle and effective natural deodorant is formulated with the botanicals sage and lemongrass to effectively combat odor, while soothing the skin with aloe vera. It provides reliable odor protection with its mild formula. We have carefully chosen a pleasant fragrance that is also gentle, and we are proud to say that our product is free from artificial preservatives, colors, and harsh alcohol. Rest assured, our deodorant contains no animal ingredients, has not been tested on animals, and is completely free from artificial additives.

Llama2
Our natural deodorant harnesses the power of sage and lemongrass to effectively combat odor, while soothing the skin with aloe vera. Our mild formula provides reliable odor protection without any harsh chemicals, artificial preservatives, or animal by-products. We've carefully selected the fragrance to be both pleasant and gentle, ensuring a comfortable and natural experience for your skin.

Mistral
This natural deodorant harnesses the power of sage and lemongrass to combat odor, while aloe vera soothes the skin. Formulated for gentle and effective use, it provides dependable protection against body odor. Free from artificial preservatives, colors, and harsh alcohol, the fragrance is derived from natural sources and is kind to sensitive skin. Cruelty-free and vegan, this deodorant does not contain any animal ingredients or undergo animal testing.

Gemini-Pro
Harnessing the power of botanicals, our natural deodorant effectively combats odor with sage and lemongrass while soothing the skin with aloe vera. Its gentle formula provides reliable protection without compromising skin health. The carefully curated fragrance ensures a pleasant scent, and our commitment to natural ingredients means no artificial preservatives, colors, or harsh alcohol. We believe in cruelty-free practices, using no animal ingredients or testing.

Table 9: Examples of HGC and AIGC on Beauty dataset.

Human

Mother's Special Blend All Natural Skin Toning Oil, a product for that special time; before, during and after pregnancy; to tone skin and help prevent stretch marks. Its rich, natural ingredients are almond oil, pecan oil, coconut oil, cocoa butter and vitamin E. Our cocoa butter is carefully selected and refined. Also can be used for toning skin during weight loss and fitness programs. Excellent for massage.

ChatGPT

Introducing Mother's Special Blend, an all-natural oil specially formulated for the unique stages of pregnancy. This remarkable product is designed to tone the skin and aid in the prevention of stretch marks, making it ideal for use before, during, and after pregnancy. Crafted with a luxurious blend of nourishing ingredients, including almond oil, pecan oil, coconut oil, cocoa butter, and vitamin E, our formula is carefully crafted to provide the utmost care for your skin. Our cocoa butter is meticulously selected and refined to ensure the highest quality. Additionally, this versatile oil can also be used to tone the skin during weight loss and fitness programs, making it a perfect companion for your wellness journey. Experience the excellence of Mother's Special Blend, perfect for indulgent massages and promoting overall skin health.

Llama2

Mother's Special Blend All Natural Skin Toning Oil is a versatile product designed to cater to various skin concerns, particularly during pregnancy. Its blend of rich, natural ingredients, including almond oil, pecan oil, coconut oil, cocoa butter, and vitamin E, work together to tone skin and prevent stretch marks. The cocoa butter used in the product is of high quality and carefully refined to ensure maximum effectiveness. Additionally, the oil can be used for toning

Mistral

Mother's Special Blend All Natural Skin Toning Oil is an essential product for pregnant women, as well as those undergoing weight loss and fitness programs. This oil, formulated for use before, during, and after these life transitions, is enriched with natural ingredients including almond oil, pecan oil, coconut oil, cocoa butter, and vitamin E. Our meticulously selected and refined cocoa butter, combined with these other nourishing elements, helps tone the skin and prevent stretch marks. Ideal for massage use.

Gemini-Pro

Mother's Special Blend All Natural Skin Toning Oil is a nourishing solution for skin care during pregnancy, weight loss, and fitness journeys. Its rich blend of almond oil, pecan oil, coconut oil, cocoa butter, and vitamin E deeply moisturizes and tones the skin, helping to prevent stretch marks and improve skin elasticity. The carefully selected and refined cocoa butter provides exceptional hydration and nourishment. This versatile oil can also be used for massage, offering a relaxing and rejuvenating experience.

Table 10: Examples of HGC and AIGC on Sports dataset.

Human

Offering 10 great exercises in a single easy-to-use machine, the Gazelle Freestyle burns calories, tones your muscles, and improves your cardiovascular endurance. The Freestyle is ideal for all fitness levels, with an unsurpassed range of motion that lets you go from a slow walk to a full run with no sudden stops, so you won't put undue pressure on your joints. The resulting aerobic workout will thus challenge you without sacrificing your knees. Details include an easy-to-use workout computer that delivers immediate feedback on speed, distance, time, and approximate calories burned; a built-in thumb pulse monitor for tracking your heart rate; extra-wide, non-skid foot platforms; a foldable footprint for easy storage; a maximum weight capacity of 300 pounds; and a personal trainer video that puts you one-on-one with Tony Little.

ChatGPT

The Gazelle Freestyle is a versatile exercise machine that offers 10 effective workouts in one convenient package. This machine is designed to help you burn calories, tone your muscles, and enhance your cardiovascular endurance. It caters to individuals of all fitness levels, thanks to its exceptional range of motion. With the Gazelle Freestyle, you can smoothly transition from a leisurely walk to a vigorous run without any abrupt stops, ensuring that your joints remain free from unnecessary strain.

Llama2

The Gazelle Freestyle is a versatile exercise machine that offers 10 effective workouts in one convenient device. It targets multiple muscle groups, improves cardiovascular endurance, and burns calories, all while being gentle on joints. The machine features an easy-to-use workout computer that tracks speed, distance, time, and estimated calories burned, as well as a built-in heart rate monitor for precise monitoring. The extra-wide foot platforms provide a stable workout surface, and the foldable design makes storage easy. With a maximum weight capacity of 300 pounds and a personal trainer video featuring Tony Little, this machine is suitable for users of all fitness levels.

Mistral

The Gazelle Freestyle machine provides a versatile workout experience, incorporating ten effective exercises in one convenient design. Suitable for various fitness levels, this equipment offers a seamless transition from a leisurely walk to a high-intensity run, minimizing joint strain due to its unmatched range of motion. The Freestyle's aerobic workout enhances calorie burning, muscle toning, and cardiovascular improvement without compromising your joints. Key features include an intuitive workout computer displaying speed, distance, time, and estimated calorie consumption; a built-in heart rate monitor with thumb pulse sensor; expansive, non-slip foot platforms; a compact, foldable design for effortless storage; a maximum weight capacity of 300 pounds; and a personal training video featuring Tony Little for one-on-one guidance.

Gemini-Pro

The Gazelle Freestyle is a versatile exercise machine that provides a comprehensive workout. It offers 10 exercises, including walking, running, and elliptical motions, catering to all fitness levels. Its unique design allows for a smooth transition between exercises, minimizing joint strain. The Freestyle features an intuitive workout computer that tracks speed, distance, time, and calories burned. Additionally, it includes a thumb pulse monitor for heart rate monitoring, extra-wide foot platforms for stability, and a foldable design for convenient storage. With a maximum weight capacity of 300 pounds, the Freestyle is suitable for a wide range of users. A personal trainer video is also included, providing expert guidance and motivation.